STEM CELLS AND DEVELOPMENT
Volume 24, Number 13, 2015

DOI: 10.1089/scd.2014.0490

Transplanted Umbilical Cord Mesenchymal Stem Cells Modify the In Vivo Microenvironment Enhancing Angiogenesis and Leading to Bone Regeneration

Maria Rosa Todeschi,[1] Rania El Backly,[1,2] Chiara Capelli,[3] Antonio Daga,[4] Eugenio Patrone,[5] Martino Introna,[3] Ranieri Cancedda,[1,4] and Maddalena Mastrogiacomo[1,4]

Umbilical cord mesenchymal stem cells (UC-MSCs) show properties similar to bone marrow mesenchymal stem cells (BM-MSCs), although controversial data exist regarding their osteogenic potential. We prepared clinical-grade UC-MSCs from Wharton's Jelly and we investigated if UC-MSCs could be used as substitutes for BM-MSCs in muscoloskeletal regeneration as a more readily available and functional source of MSCs. UC-MSCs were loaded onto scaffolds and implanted subcutaneously (ectopically) and in critical-sized calvarial defects (orthotopically) in mice. For live cell-tracking experiments, UC-MSCs were first transduced with the luciferase gene. Angiogenic properties of UC-MSCs were tested using the mouse metatarsal angiogenesis assay. Cell secretomes were screened for the presence of various cytokines using an array assay. Analysis of implanted scaffolds showed that UC-MSCs, contrary to BM-MSCs, remained detectable in the implants for 3 weeks at most and did not induce bone formation in an ectopic location. Instead, they induced a significant increase of blood vessel ingrowth. In agreement with these observations, UC-MSC-conditioned medium presented a distinct and stronger proinflammatory/chemotactic cytokine profile than BM-MSCs and a significantly enhanced angiogenic activity. When UC-MSCs were orthotopically transplanted in a calvarial defect, they promoted increased bone formation as well as BM-MSCs. However, at variance with BM-MSCs, the new bone was deposited through the activity of stimulated host cells, highlighting the importance of the microenvironment on determining cell commitment and response. Therefore, we propose, as therapy for bone lesions, the use of allogeneic UC-MSCs by not depositing bone matrix directly, but acting through the activation of endogenous repair mechanisms.

Introduction

Bone marrow mesenchymal stem cells (BM-MSCs) are considered the gold standard cell population in bone engineering and regenerative medicine applications [1]. The implantation of these cells combined with ceramic-based biomaterials in bone defects gives the best results in terms of bone formation both in animal models [2,3] and in patients [4]. Although BM-MSCs are a feasible and autologous source of MSCs, their painful and invasive collection method has limited their use. Moreover, BM-MSCs are adult stem cells with lower proliferation capacity compared with other MSCs originating from fetal tissues [5]. The umbilical cord (UC) can be a source of highly proliferating fetal MSCs [6,7] that are more easily collectable than BM-MSCs. UC-MSCs are isolated from Wharton's Jelly, representing a noncontroversial source of fetal stem cells [8]. Because of their fetal origin, nowadays, the use of UC-MSCs in an allogeneic system is almost the only application for them. UC-MSCs have great immunomodulation capacity [9]; they act on the innate immunity by inhibiting the maturation and the activation of dendritic cells [10], the activation of the $CD56^{dim}$ NK subpopulation, and NK cytotoxicity [11]. Moreover, UC-MSCs have an influence on adaptive immunity by blocking T cell proliferation [9,10] and modulating B cell proliferation and differentiation [12,13]. Thus, UC-MSCs have become an appealing cell source for treatment of diseases where inflammation plays a crucial role such as graft-versus-host disease [14] (www.clinicaltrials.gov; Identifier: NCT02032446). Indeed, fetal MSCs have been shown to possess stronger immunomodulation properties and lower immunogenicity than adult MSCs [15,16]. In view of a rapid

[1]Department of Experimental Medicine (DIMES) and [5]Department of Prosthetic Dentistry, University of Genoa, Genoa, Italy.
[2]Faculty of Dentistry, Alexandria University, Alexandria, Egypt.
[3]A.O.Papa Giovanni XXIII-USS Center of Cell Therapy ''G. Lanzani'' USC Hematology, Bergamo, Italy.
[4]IRCCS AOU San Martino-IST National Cancer Research Institute, Genoa, Italy.

increase in the use of UC-MSCs in the clinic, protocols of cell isolation and expansion under good manufacturing practice (GMP) guidelines are being developed.

In this context, we prepared clinical-grade UC-MSCs [6], and we investigated if UC-MSCs could be used as substitutes for BM-MSCs in musculoskeletal regeneration. UC-MSCs clearly display typical MSC features as defined by the International Society for Cellular Therapy [17]. Both UC-MSCs and BM-MSCs are plastic adherent and show similar cell surface marker expression. Interestingly, the only major difference is their differentiation potential [6]. UC-MSCs have a very weak osteogenic [18–20], chondrogenic [21], and adipogenic [19,20] differentiation capacity compared with BM-MSCs. The reasons for these differences need to be further clarified, but it has been postulated that the reduced differentiation potential of UC-MSCs may depend on their position within the UC tissue they are isolated from [22]. As the cells in the human UC stroma are not uniformly distributed, it may be hypothesized that, depending on the isolation technique used, slightly different types of primitive cells with unequal differentiation capabilities can be obtained [6]. It must also be taken into consideration that whereas BM-MSCs may be more committed to osteogenesis because of their natural density in the bone and in maintaining the self-renewal capacity of hematopoietic stem cells, UC-MSCs having a fetal origin might require stronger inductive stimuli or more time to differentiate into a specific tissue [23,24].

Increasing evidence has also recently suggested a predominant paracrine role of MSCs in promoting tissue regeneration due to their secretome enriched in proinflammatory, chemotactic, and angiogenic factors rather than due to their direct replacement of affected cells at the site of injury [25]. Additionally, since vascularization is a crucial aspect in the tissue regeneration process, this inherent characteristic of MSCs, particularly of UC-MSCs, would be interesting to explore.

Hence, to better clarify the potential of UC-MSCs in regenerative medicine and to compare them with BM-MSCs in an in vivo osteogenic environment, we wanted to answer the following questions:

1. Can an osteogenic environment, whether ectopic or orthotopic, influence the osteogenic regenerative capacity of UC-MSCs expanded according to a clinical-grade protocol?
2. Are the regenerative effects of implanted UC-MSCs attributed to their direct engraftment or could their paracrine/trophic effects be responsible?
3. Can UC-MSCs mediate a therapeutic angiogenic response, thus leading to enhanced bone regeneration?

Materials and Methods

Cell isolation and culture

Human UC-MSC culture. Human UCs were collected from pregnant women after cesarean sections. Informed written consent was obtained. The UC processing was performed in accordance with a GMP-compliant protocol for the isolation and expansion of UC-MSCs [6]. Briefly, the UC was cut into segments, which were split open to expose the inner surface. The UC segments were transferred to an expansion medium, consisting of alpha-minimum essential medium with GlutaMAX™ (Invitrogen) enriched with 5% human platelet lysate (PL) obtained from healthy donors, 2 IU/mL Na-heparin (Epsoclar; Hospira s.r.l.), and 100 μg/mL streptomycin (Sigma Chemical Co.), and minced. Minced pieces were incubated in the expansion medium at 37°C and 5% CO_2 for 1 week to allow the cells to adhere, and then they were removed. At 80% confluence, the cells were detached by treatment with Tryple (Invitrogen) and passaged. All experiments were performed using at least three different primary cultures at either P1 or P2.

Human BM-MSC culture. Human BM-MSCs were obtained from iliac crest marrow aspirates of healthy bone marrow transplant donors after informed consent. The BM-MSCs were cultured in complete culture medium consisting of Coon's modified Ham's F-12 medium containing 2 mM glutamine, 100 IU/mL penicillin, 100 μg/mL streptomycin (Sigma Chemical Co.), and 10% fetal bovine serum (FBS; Invitrogen) in the presence of 1 ng/mL human recombinant fibroblast growth factor-2 (FGF-2; Peprotech). At 80% confluence, the cells were detached by treatment with 0.05% trypsin −0.01% ethylenediaminetetraacetic acid (EDTA; Sigma Chemical Co.) and passaged. All experiments were performed using at least three different primary cultures at either P1 or P2.

Conditioned medium preparation. The conditioned medium (CM) was collected from 80% confluent cultures of either UC-MSCs or BM-MSCs in 10-cm tissue culture dishes. Each culture dish received 7 mL of serum-free media for 48 h. The CM was collected by centrifugation at 440 *g* for 5 min and by a second centrifugation at 1,750 *g* for 3 min, both centrifugations were at 4°C [26].

Platelet lysate preparation. Whole blood was collected from voluntary donors following current procedures for blood donation. Blood units were screened for the absence of infectious agents in compliance with national regulatory requirements. Buffy coats (BC) were obtained by centrifugation of whole blood donations. Five BC units were pooled, platelet-rich plasma (PRP) separated by light-spin centrifugation, and the platelets concentrated by a second heavy-spin centrifugation. PRP was resuspended in homologous plasma and stored at −30°C. The standard PRP unit had a platelet concentration of $1–2 \times 10^6$/μL. PL was obtained by subjecting PRP to three cycles of freezing and thawing. The PL was aliquoted and stored at −20°C.

Ectopic bone formation assay

All experimental animal procedures were evaluated and approved by the IRCCS AOU San Martino-IST Ethics Committee for animal experimentation (CSEA) and communicated to the Italian Ministry of Health in accordance with article 7 of the D.lgs 27/01/1992 n.116/92.

The in vivo analysis was based on an established model of ectopic bone formation [27]. Briefly, we prepared the implantable constructs by seeding 2.5×10^6 UC-MSCs onto ceramic scaffolds (Skelite; 4 × 4 × 4 mm cubes of 33% hydroxyapatite and 67% silicon-stabilized tricalcium phosphate, Si-TCP) and embedding the scaffolds in a fibrin glue (Tissucol; Baxter). Moreover, nonseeded empty Skelite and Skelite seeded with 2.5×10^6 BM-MSC constructs were used as negative and positive control groups, respectively ($n = 4$).

Scaffolds were implanted subcutaneously on the dorsal surface of immunocompromised mice (CD-1 Nu/Nu; Charles River). The implants were recovered at 60 days and histologically analyzed.

Histological analysis

Harvested samples were fixed in 3.7% paraformaldehyde, decalcified in EDTA 10%, and paraffin embedded. Sections were cut at 4 μm thickness and stained with hematoxylin and eosin (H&E) and Masson's trichrome (MTC) (Masson's trichrome special staining kit; Bio-Optica) stains. Moreover, chromogenic in situ hybridization (Zytovision kit) to detect human ALU repeat sequences was performed following the manufacturer's instructions. Images of the sections were acquired using a phase-contrast Axiovert 200M microscope (Zeiss). Polarized light images were acquired using a phase-contrast Axiophot microscope (Zeiss).

The number of blood vessels in the ectopic implants ($n=3$) was manually counted in multiple, representative MTC-stained sections for UC-MSCs and BM-MSC-seeded and empty scaffolds (six per condition per experiment). The bone surface area in the orthotopic implants ($n=3$) was manually measured in multiple representative H&E-stained sections for all groups. Three sections per condition per experiment were analyzed. The ratio between the neoformed bone area and total defect area was calculated for each section.

To perform the histologic quantification analysis, ImageJ (NIH) software was used.

In vivo live cell-tracking analysis

To perform live cell-tracking experiments, UC-MSCs and BM-MSCs were transduced using a replication-incompetent amphotropic bicistronic retrovirus encoding the firefly luciferase gene (Luc) [28]. Retroviral vectors and infection protocols were performed as previously described [29]. Luc-infected UC-MSCs and BM-MSCs were selected by adding G418 (Gibco) at 0.5 mg/mL to the medium for 10 days. MSC-transduced cells (2.5×10^6) were seeded onto Skelite scaffolds and implanted as reported above.

The in vivo bioluminescence reaction induced by the substrate luciferin (150 mg/kg; D-Luciferin Firefly Xenogen) injections in mice was detected using the IVIS® Imaging System LUMINA II (PerkinElmer) ($n=3$ in BM-MSC implants and $n=6$ in UC-MSC implants). Mice were imaged for 5 min after 1, 7, 21, and 30 days postimplantation.

Metatarsal angiogenesis assay

The metatarsal angiogenesis assay was performed as previously described [30]. Briefly, metatarsals of 17-day-old, wild-type mouse embryos (FVB/N; Charles River) were transferred to culture dishes to allow their attachment for 72 h. Bones were then cultured for 13 days with either UC-MSC CM or BM-MSC CM, both implemented with 10% FBS. Fresh complete medium containing 10% FBS was used as the experiment control. After 13 days of culture, bones were fixed and stained for PECAM-1/CD31. Quantification of the number of CD31 positively stained pixels and the outgrowth area from bone were performed using ImageJ (NIH) software ($n=3$).

Proteomic identification and bioinformatics analysis

Cytokine screening of UC-MSC secretome was performed on CM using a human cytokine array (Panel A; R&D Systems) following the manufacturer's instructions. The cytokines identified in the CM of UC-MSCs were uploaded into the web-based DAVID platform (www.david.abcc.ncifcrf.gov). The protein list was analyzed by clusterization into Gene Ontology (GO) biological processes.

Assessment of bone formation in the mouse calvarial defect

Discs of nanohydroxyapatite/poly (ester urethane) (nHA/PU) with a diameter of 5 mm and height of 2 mm were provided by the AO Research Institute (Davos, Switzerland). These scaffolds have been shown to support orthotopic bone formation in a rabbit model [2]. Immediately before surgery, 2.5×10^6 UC-MSCs were loaded onto the scaffolds and embedded in a fibrin glue (Tissucol; Baxter). Moreover, nonseeded empty nHA/PU discs and discs seeded with 2.5×10^6 BM-MSC constructs were used as negative and positive control groups, respectively ($n=3$).

The constructs were implanted in 5-mm critical-size defects in the calvaria of immunocompromised mice (CD-1 Nu/Nu; Charles River).

The critical-sized calvarial defects were made as previously described in the literature [31]. Mice were anesthetized with ketamine (80–100 mg/kg) and xylazine (5–10 mg/kg). A 5-mm defect was prepared in the center of the parietal bones of each mouse calvarium using Mectron Piezosurgery® instruments (Mectron s.p.a.). The construct was then carefully placed and the flap was repositioned and sutured using 4.0 vicryl (Ethicon) suture material. The implants were recovered 90 days postoperatively, decalcified, and then histologically analyzed.

Statistical analysis

The results are expressed as mean and standard error of the mean. Statistical significance was determined using the ordinary one-way ANOVA and the value of $P<0.05$ was considered to be statistically significant. Statistical analysis was performed by Graphpad software.

Results

UC-MSC behavior in an ectopic bone formation model

Histological assessment of the tissues formed within the ectopically implanted scaffolds revealed the formation of mature bone in the pores of the scaffolds seeded with BM-MSCs (Fig. 1E), whereas UC-MSC-seeded constructs showed a compact fibrous tissue ascribable to an immature bone-like structure (Fig. 1F). In the nonseeded implants, a loose connective fibrous tissue was observed (Fig. 1D). Polarized light examination confirmed the presence of highly organized collagen fibers in the BM-MSC-seeded implants (Fig. 1H) compared with the weaker signal observable in the UC-MSC-seeded scaffolds (Fig. 1I). In the nonseeded scaffold samples, no polarized light signal was detected (Fig. 1G).

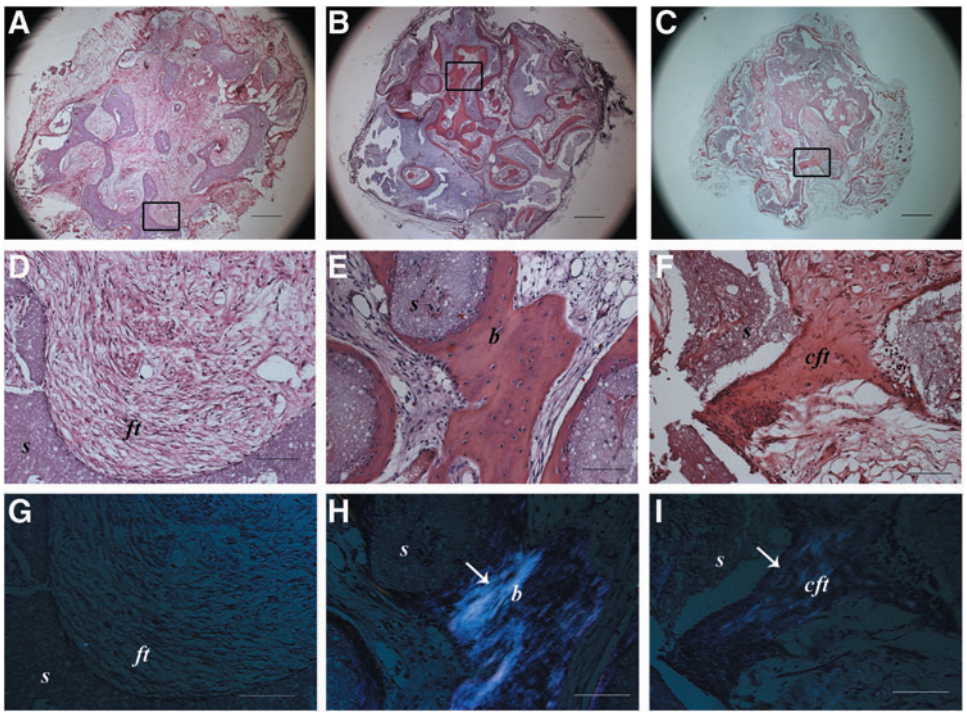

FIG. 1. Histological images of ectopic implants after 2 months and stained with hematoxylin and eosin **(A–F)** and analyzed by polarized light **(G–I)**. *Black rectangles* indicate the areas from which higher magnification images where taken. **(A, D, G)** non-cell-seeded empty scaffold; **(B, E, H)** bone marrow mesenchymal stem cell (BM-MSC)-seeded scaffolds; **(C, F, I)** umbilical cord mesenchymal stem cell (UC-MSC)-seeded scaffolds. *s*, scaffold; *ft*, fibrous tissue; *b*, bone; *cft*, compact fibrous tissue; (↑), polarized light signal. Scale bars = 600 μm **(A–C)** and 100 μm **(D–I)**. ($n = 4$ for both cell-seeded and not seeded scaffold groups). Color images available online at www.liebertpub.com/scd

Low-magnification micrographs (Fig. 1A–C) showed that the bone tissue in BM-MSC-seeded scaffolds was formed in most of the area of the implant (Fig. 1B), whereas in UC-MSC-seeded scaffolds, the immature bone-like matrix was sparsely present (Fig. 1C) with the majority of the area filled with a loose connective tissue similar to that seen completely filling the nonseeded scaffolds (Fig. 1A).

UC-MSC angiogenic effect in vivo

Although only a minimal amount of immature bone-like matrix could be detected in the UC-MSC-seeded scaffolds, an accurate analysis of these implants revealed an abundance of blood vessels (Fig. 2C) compared with the BM-MSC-seeded (Fig. 2B) and empty implants (Fig. 2A). The characteristic gold staining of the MTC stain revealed the presence of red blood cells in most of the vessel-like structures (Fig. 2A–C). Quantitative analysis confirmed the presence of a significantly higher number of blood vessels in UC-MSC implants than in either BM-MSC-seeded ($P < 0.0001$) or empty scaffolds ($P < 0.0001$) (Fig. 2D).

In situ hybridization analysis showed that there was no positive signal for human ALU repeat sequences detected in any area of the 2-month UC-MSC implants, including the fibroblasts forming the compact fibrous tissue and the endothelial cells lining the vessel structures. Therefore, based on

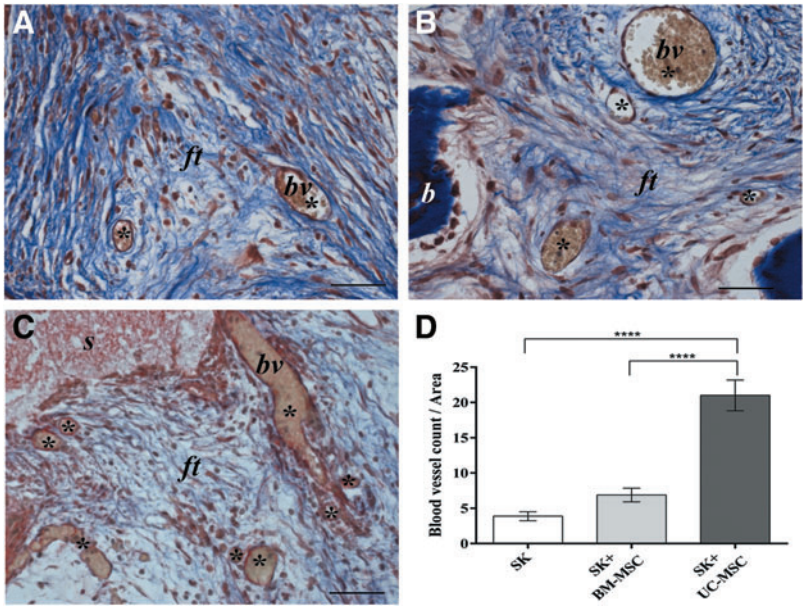

FIG. 2. Histological images of ectopic implants recovered after 2 months and stained with Masson's trichrome showing a high number of blood vessel-like structures in the UC-MSC-seeded scaffold **(C)** compared with the BM-MSC-seeded scaffold **(B)** and empty scaffold **(A)**. *bv*, blood vessel; *ft*, fibrous tissue; *b*, bone; (*), blood vessel count. Scale bar = 100 μm. ($n = 4$ for both cell-seeded and not seeded scaffold groups). In **(D)** a quantification of the number of blood vessels present in 2-month implants of the empty scaffold (SK) and BM-MSC and UC-MSC-seeded scaffolds (SK + BM-MSC and SK + UC-MSC) is presented. (****$P <$ 0.0001). Color images available online at www.liebertpub.com/scd

this observation, we classified the immature bone-like structure (Fig. 3E, F) and the neoformed vessels of murine origin (Fig. 3G, H). On the contrary, the mature bone formed in BM-MSC implants was undoubtedly of human origin. Cells derived from implanted human BM-MSCs were evident both in the newly formed bone as osteoblasts and osteocytes and in the fibrous tissue as fibroblast-like cells (Fig. 3C, D). As expected, no signal for ALU sequences was detected in the nonseeded implants (Fig. 3A, B).

In vivo permanence of UC-MSCs

In light of the previous evidence, we performed live cell-tracking analysis by detecting the light signal produced by transduced MSCs. The bioluminescent signal produced by UC-MSCs drastically decreased over time and completely disappeared by 1 month (Fig. 4B). On the contrary, the BM-MSC bioluminescent signal remained detectable throughout the entire testing period (Fig. 4A).

UC-MSC secretome induces angiogenesis in vitro

In light of the previous data, we investigated whether the UC-MSC secretome (CM) alone could induce angiogenesis in a functional in vitro assay. Indeed, a widespread sprouting of blood vessels from fetal bone was induced by UC-MSC CM (Fig. 5C). On the contrary, BM-MSC CM showed a poor effect on inducing the formation of new blood vessels and behaved similar to the fresh medium controls (CTR) (Fig. 5A, B). UC-MSC CM significantly enhanced the number of PECAM/CD31-stained cells (vs. CTR $P<0.05$; vs. CM BM-MSC $P<0.05$) (Fig. 5D) as well as the area of

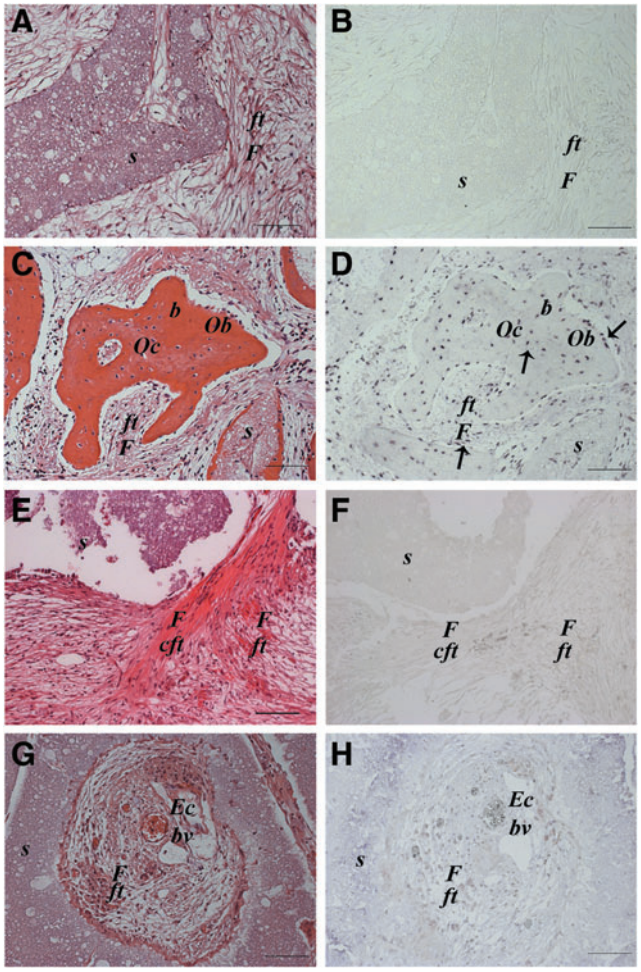

FIG. 3. Histological images of ectopic implants recovered after 2 months and stained with hematoxylin and eosin **(A, C, E, G)** and analyzed by in situ hybridization for the human ALU repeat sequence **(B, D, F, H)**. Empty scaffold (SK) **(A, B)**; BM-MSC-seeded scaffold osteocytes and osteoblasts of human origin are present. Moreover, human cells are detectable and also found in the fibrous tissue as fibroblasts **(C, D)**; UC-MSC-seeded scaffold. No human cells present in the compact fibrous tissue **(E, F)** and in the blood vessel endothelium **(G, H)**. *s*, scaffold; *F*, fibroblast; *ft*, fibrous tissue; *cft*, compact fibrous tissue; *Oc*, osteocyte; *Ob*, osteoblast; *b*, bone; *Ec*, endothelial cell; *bv*, blood vessel; (↑), human cell. Scale bar = 100 μm. ($n=4$). Color images available online at www.liebertpub.com/scd

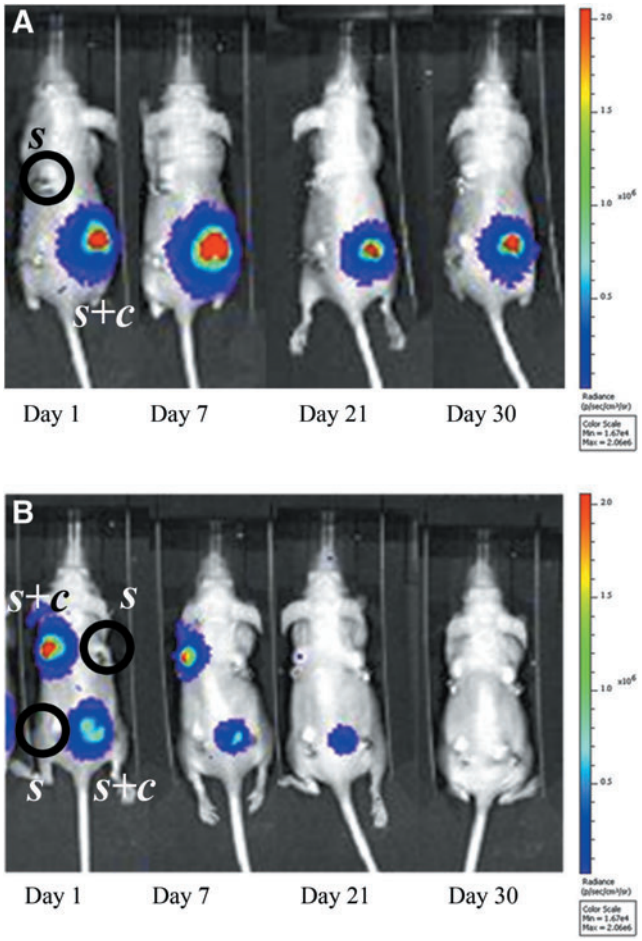

FIG. 4. In vivo bioluminescence imaging, at different time points after surgery, of mice ectopically implanted with scaffolds seeded with cells ($s+c$) or not seeded (s). A decreasing signal is noticeable for UC-MSC-seeded scaffolds **(B)**, whereas the signal for the BM-MSC-seeded scaffold remains stable throughout the whole observation time **(A)**. No signal is detected in empty scaffolds **(A, B)**. ($n=6$ for both UC-MSC-seeded and not seeded scaffold groups, and $n=4$ for the BM-MSC-seeded scaffold group). Color images available online at www.liebertpub.com/scd

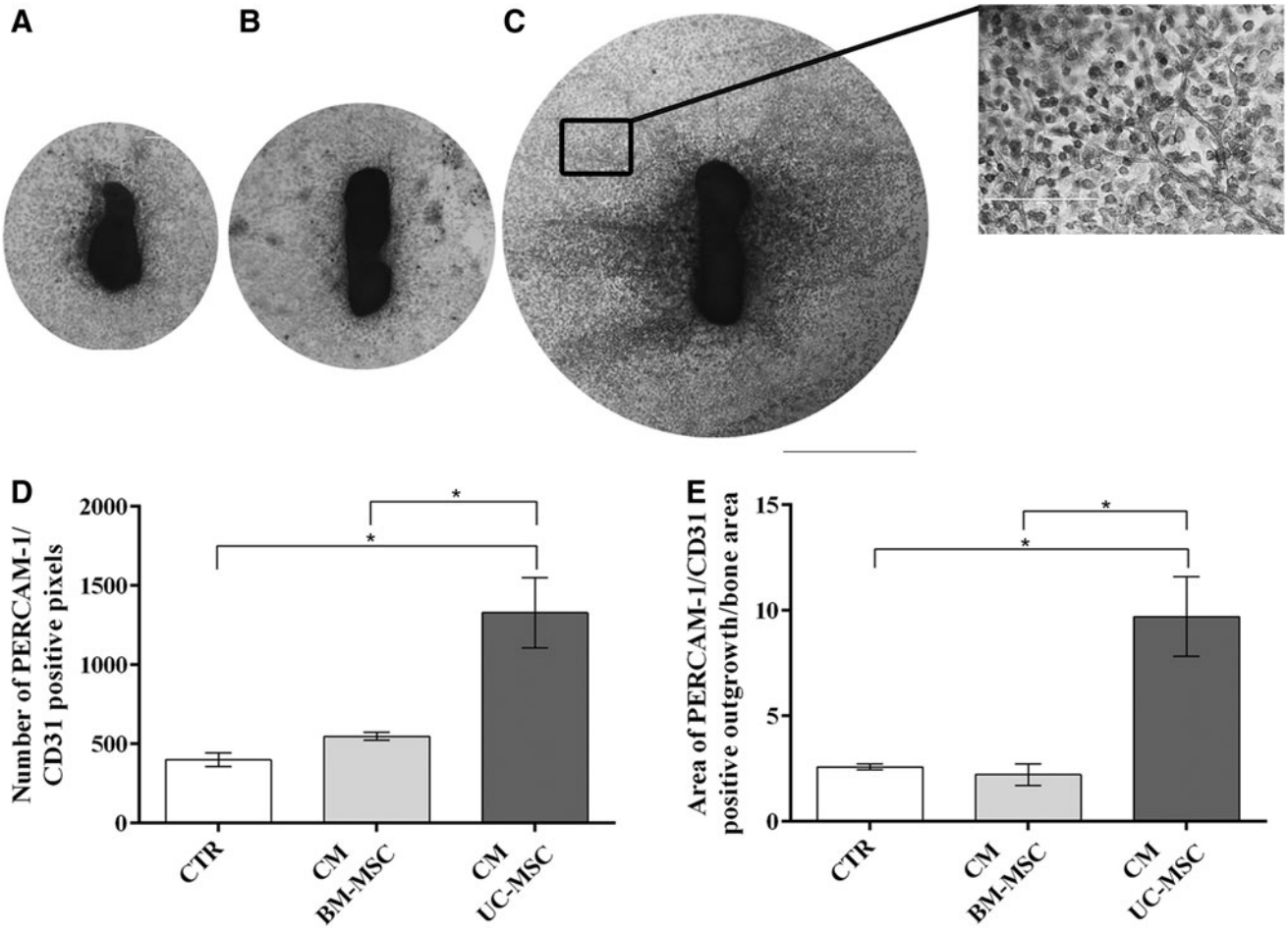

FIG. 5. Blood vessel sprouting in explants of mouse fetal metatarsal bones maintained in different culture conditions. Vessels were stained with antibodies against PECAM-1/CD31. Explants were cultured in the presence of **(A)** control medium (CTR); **(B)** BM-MSC-conditioned medium (BM-MSC CM); and **(C)** UC-MSC-conditioned medium (UC-MSC CM). Scale bar = 1,000 μm **(A–C** and **C** *insert*). Quantification of the number of PECAM-1/CD31-positive pixels and the area of vessel outgrowth are shown in **(D, E)**, respectively. (*$P < 0.05$) ($n = 3$ for both cell CM and control medium).

vessel outgrowth when compared with the other conditions (vs. CTR $P < 0.05$; vs. CM BM-MSC $P < 0.05$) (Fig. 5E).

UC-MSC secretome is rich in proinflammatory, proangiogenic, and chemotactic cytokines

We addressed the possible paracrine effects of UC-MSCs by investigating their secretome. Numerous cytokines were secreted by UC-MSCs (Fig. 6B). Most of the ones present in a high amount (IL-6, IL-8, CCL2, PAI-1, CXCL1, MIF, and G-CSF) (Fig. 6C) are known to be involved in the modulation of the inflammatory process. These cytokines were not secreted by BM-MSCs or their level in the CM was much lower than in UC-MSC CM. PAI-1 was the only cytokine secreted in a relatively significant amount by BM-MSCs in the same conditions (Fig. 6A, C).

Bioinformatic analysis performed in GO gave information about the biological processes involving the screened cytokines. The prevalent biological functions recorded concerned the activation of angiogenesis, cell signaling, cell proliferation, chemotaxis, tissue repair/regeneration, modulation of leukocytes, and inflammation. Each of these biological processes involved two to nine of the screened cytokines.

The first four biological processes that emerged by the analysis are strictly related to generic cytokine roles; therefore, we excluded the first four GO term scores (gray rows) from the evaluation (Table 1).

UC-MSC-induced bone formation by the host cells in an orthotopic mouse model

Histological evaluation of the 90-day recovered orthotopic implants showed that none of the bone defects from any of the three groups had completely closed (Fig. 7A–C). However, abundant, newly formed mature bone tissue was observed in the defects that received BM-MSC-seeded scaffolds (Fig. 7B). Nevertheless, a good amount of mature bone was also observed in the defects filled with UC-MSC-seeded scaffolds (Fig. 7C). In the defects that received noncell-seeded scaffolds, only a small amount of new bone tissue was noted (Fig. 7A, D). An analysis using polarized light highlighted the presence of abundant bone tissue with highly organized fibers in BM-MSC-seeded implants (Fig. 7B). In UC-MSC-seeded implants, the polarized light revealed less extended and less defined fibers (Fig. 7C). A negligible signal was detected in nonseeded implants (Fig.

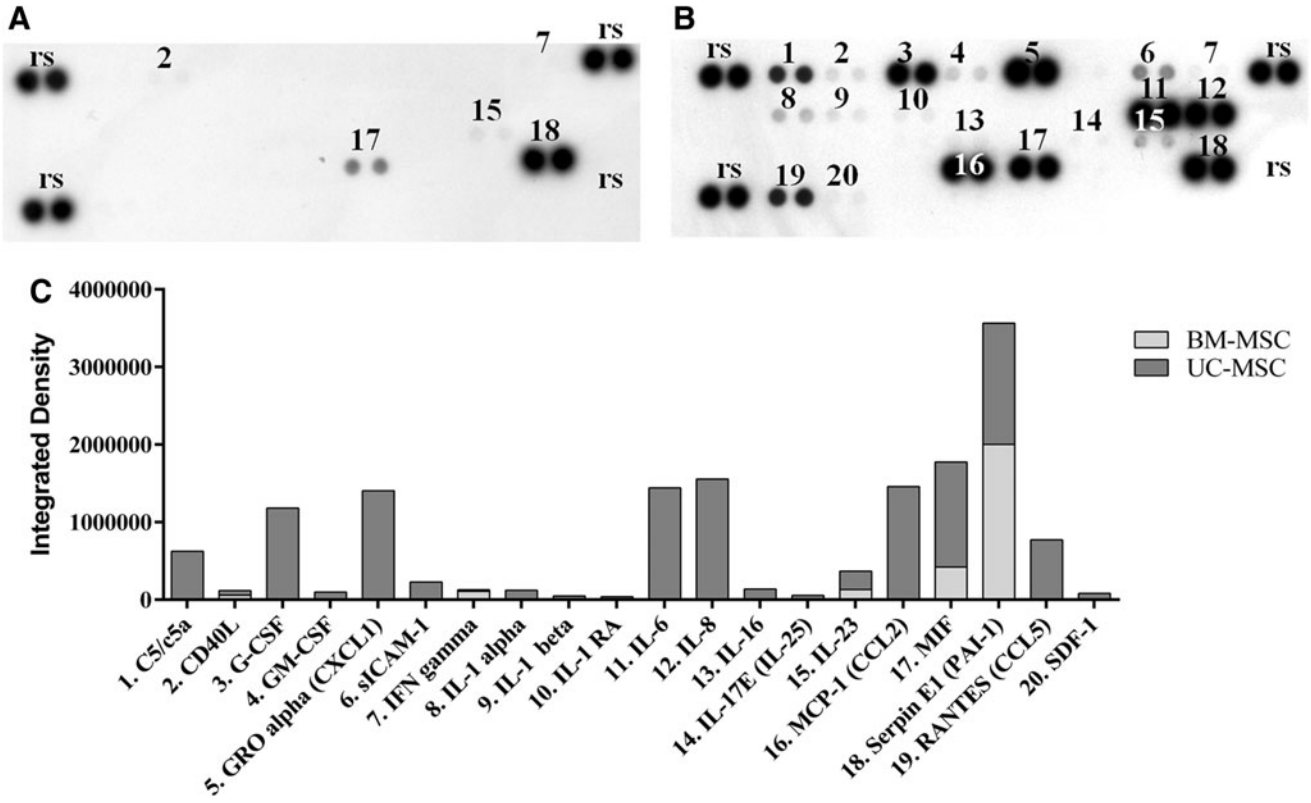

FIG. 6. Cytokine array membrane assay of MSC CM; **(A)** BM-MSC CM; **(B)** UC-MSC CM; **(C)** quantification of the positive pixels for each identified cytokine in BM-MSC and UC-MSC CM. rs, reference spots represent an internal control.

7A). There were no significant differences in the amounts of new bone filled between BM-MSC and UC-MSC groups ($P = 0.97$). However, it was significantly higher in both groups with respect to the nonseeded controls (CTR vs. UC-MSC $P < 0.0001$; CTR vs. BM-MSC $P < 0.001$) (Fig. 7D).

To determine the origin of the regenerated bone, in situ hybridization analysis of human ALU sequences was performed. Similar to what was demonstrated in the ectopic implants, in the BM-MSC-seeded scaffolds, osteocytes of human origin were clearly detectable (Fig. 7F), indicating that the seeded MSCs remained in the scaffold for 3 months and successfully differentiated into viable osteoblasts that could lay down new bone matrix. On the contrary, we could not detect any signal for human ALU sequences in osteocytes within the newly formed bone in the UC-MSC implants, neither in the center (Fig. 7H) nor at the periphery (Fig. 7G) of the defect. This confirmed the murine origin of the regenerated tissue and again that UC-MSCs did not physically remain in the scaffolds. As expected, no signal was detected in the nonseeded implants (Fig. 7E).

Discussion

Despite several articles that have reported similar phenotypic characteristics for UC-MSCs and BM-MSCs, controversial data exist on their respective roles in the body's physiological tissue environments and their fate after in vitro expansion and in vivo implantation. In this work, we were mainly concerned with the osteogenic potential of in vitro-expanded UC-MSCs compared with BM-MSCs [30–32].

To obtain the cells required for the comparison of the osteogenic potential of the two MSC populations, we relied on culture protocols authorized for use in cell therapy applications (www.clinicaltrials.gov, Identifier: NCT02032446) [4]. In view of the increasing use of UC-MSCs for clinical therapy, it has become crucial to adhere to GMP guidelines for the ex vivo manipulation and expansion of these cells. Regulatory requirements strongly recommend avoiding any animal-derived medium component as FBS for cell expansion [33,34]. In this context, a GMP-compliant method was PL as a substitute for FBS. While other isolation and expansion protocols of UC-MSCs were proposed [33,35], the method we adopted allows a minimal manipulation of the UC, thus avoiding the possible initial selection of cell subpopulations [6] yielding the isolation of high-grade MSCs [36].

On the contrary, the classical expansion protocols for BM-MSCs, accepted for clinical use by the regulatory agencies [4], still employ FBS with FGF-2 as the medium additional supplement, which provides excellent results [37,38]. However, with regard to the present study, it should be noted that no major changes were observed in the phenotype characteristics and properties of BM-MSCs expanded in the presence of PL or FBS [34,36,39].

Although UC-MSCs are considered MSCs since they fulfill classical criteria [17], they do not appear as efficient as BM-MSCs for ectopic bone formation. UC-MSCs failed to deposit a well-developed bone structure, being limited to the promotion of the deposition of a dense collagen matrix. Similar results were obtained also by other research groups [32,40]. Furthermore, preinduction of UC-MSCs by

Table 1. Bioinformatics Analysis in Gene Ontology of the Screened Cytokines for Umbilical Cord Mesenchymal Stem Cell-Conditioned Medium

GO term	*Cytokine involved*																*Count*	*%*	P-*value*
Immune system process		MIF	IL-8	IL-6	IL-25	IL-23A	IL-1B	IL-IA	IL-1RA	IFNG	C5	CSF2	CXCL1	CCL5	CCL2	CD40L	15	94	1,00E-15
Response to wounding	PAI-1	MIF	IL-8	IL-6	IL-25	IL-23A	IL-1B	IL-IA	IL-1RA		C5		CXCL1	CCL5	CCL2	CD40L	14	88	2,50E-17
Defense response		MIF	IL-8	IL-6	IL-25	IL-23A	IL-1B	IL-IA	IL-1RA	IFNG	C5		CXCL1	CCL5	CCL2	CD40L	14	88	1,70E-16
Inflammatory response		MIF	IL-8	IL-6	IL-25	IL-23A	IL-1B	IL-IA	IL-1RA		C5		CXCL1	CCL5	CCL2	CD40L	13	81	7,70E-18
Regulation of cell proliferation	PAI-1		IL-8	IL-6			IL-1B	IL-IA		IFNG		CSF2	CXCL1		CCL2		9	56	4,10E-07
Locomotory behavior			IL-8	IL-6			IL-1B			IFNG	C5		CXCL1	CCL5	CCL2		8	50	5,40E-09
Negative regulation of apoptosis		MIF		IL-6			IL-1B	IL-1A				CSF2			CCL2	CD40L	7	44	9,90E-07
Cell chemotaxis			IL-8	IL-6			IL-1B			IFNG				CCL5	CCL2		6	38	3,60E-10
Localization of cell			IL-8	IL-6			IL-1B			IFNG				CCL5	CCL2		6	38	1,20E-05
Regulation of secretion				IL-6			IL-1B	IL-1A		IFNG						CD40L	5	31	4,90E-05
Cell activation			IL-8	IL-6		IL-23A						CSF2				CD40L	5	31	1,90E-04
Positive regulation of cell communication				IL-6			IL-1B			IFNG		CSF2			CCL2		5	31	3,20E-04
Regulation of angiogenesis	PAI-1			IL-6			IL-1B	IL-1A									4	25	3,70E-05
Acute inflammatory response				IL-6			IL-1B	IL-1A			C5						4	25	1,40E-04
Regulation of vascular endothelial growth factor production				IL-6			IL-1B	IL-1A									3	19	3,80E-05
Acute-phase response				IL-6			IL-1B	IL-1A									3	19	8,00E-04
Blood coagulation	PAI-1			IL-6												CD40L	3	19	5,10E-03
Leukocyte-mediated immunity				IL-6							C5					CD40L	3	19	3,70E-03
Chronic inflammatory response							IL-1B							CCL5			2	13	6,40E-03
Platelet activation				IL-6												CD40L	2	13	3,30E-02
Regeneration	PAI-1														CCL2		2	13	7,10E-02

Biological processes identified by the cytokine clusterization (activation of angiogenesis, cell signaling, cell proliferation, chemotaxis, tissue repair/regeneration, modulation of leukocytes, and inflammation) involved from two to nine of the selected cytokines. The first four GO term scores (*gray rows*) were excluded.

GO, gene ontology.

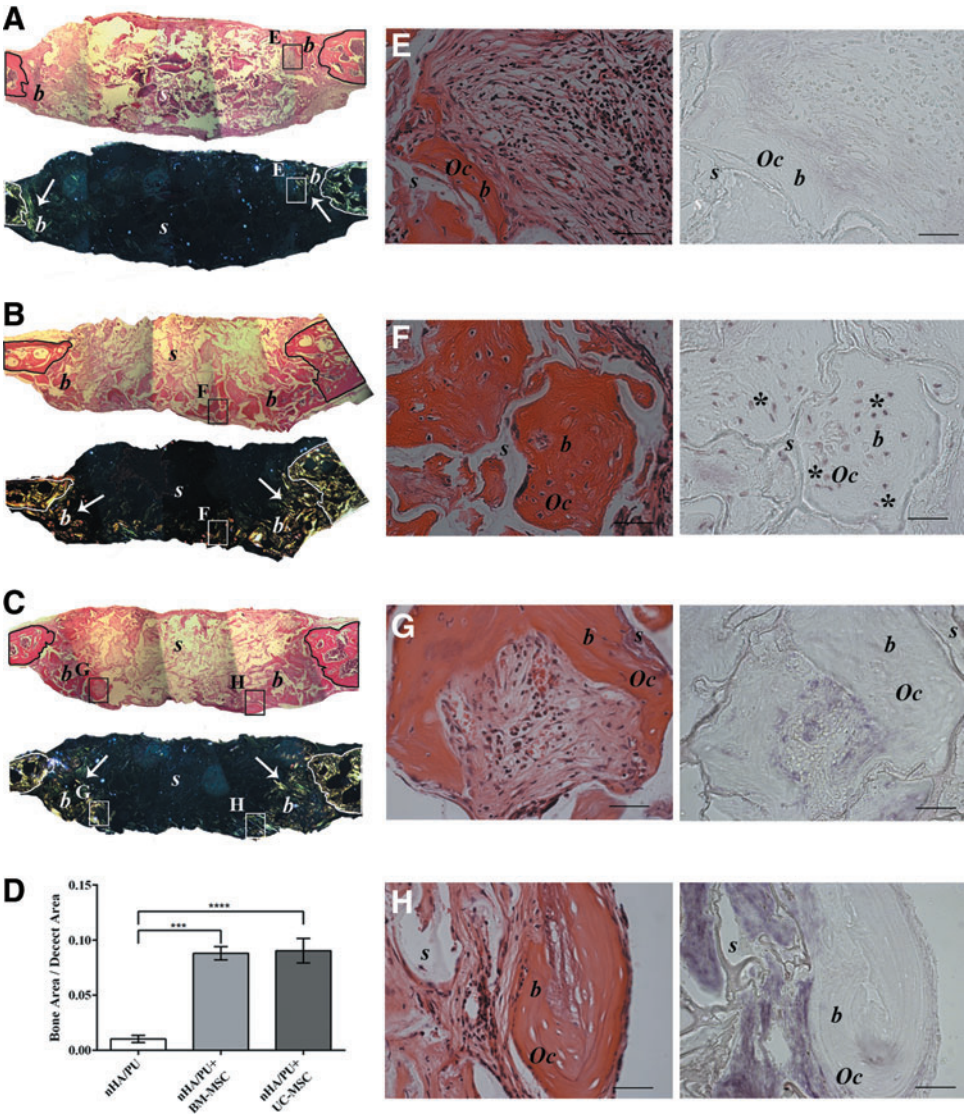

FIG. 7. Histological images of orthotopic implants in mouse calvaria recovered after 3 months, stained with hematoxylin and eosin, and analyzed by polarized light at low magnification **(A–C)** and stained with hematoxylin and eosin and analyzed by in situ hybridization for human ALU repeat sequences at high magnification **(E–H)**. *Black rectangles* indicate the areas from which higher magnification images where taken. **(A, E)** Empty scaffold (PU-HA); **(B, F)** BM-MSC-seeded scaffold (PU-HA + BM-MSC); **(C, G, H)** UC-MSC-seeded scaffold (PU-HA + UC-MSC). ($n = 3$ for both cell-seeded and not seeded scaffold groups.) A quantification of the new bone formed in each condition determinated by measuring the surface area of new bone is shown in **(D)**. *s*, scaffold; *b*, bone; (↑), polarized light signal; *Oc*, osteocyte; (*), human cell. Scale bar = 1,000 and 50 μm for **(A–C)** and **(E–H)**, respectively. ****(mHA/PU vs mHA/PU + UC-MSC $P < 0.0001$ and vs mHA/PU + BM-MSC $P < 0.001$). Color images available online at www.liebertpub.com/scd

osteogenic differentiation media, or BMP-2, did not significantly enhance their ossification potential in vivo [32,41]. The bone lack was even not influenced by the in vivo stay time (data not shown) or by the ceramic scaffold itself [42].

On the contrary, ectopically implanted BM-MSCs underwent osteogenic differentiation and deposited a true bone tissue. Interestingly, when orthotopically implanted in the mouse calvaria, both MSC populations promoted the formation of new bone; however, while bone was directly deposited by BM-MSCs, UC-MSCs did not directly deposit a bone matrix and instead triggered the recruitment of osteogenic host cells.

We showed by in situ hybridization and by flow cytometry (data not shown) that UC-MSCs remained in vivo at the implantation site only for a brief time. This observation is consistent with other published data where implanted human amniotic fluid stem cells were detected only for a few days within the implants [43]. Similarly, implanted UC-MSCs remained detectable in a skin lesion model only up to 11 days [44]. However, others have reported that ectopically implanted UC-MSCs could be detected in newly formed bone tissue after 8 weeks of implantation [45].

At variance with UC-MSCs, it is widely accepted that BM-MSCs are able to directly engraft, differentiate, and deposit new bone [40], although only 10% of the adult implanted BM-MSCs remain in the ectopic implants after 14 days [46].

Recent studies suggest that the benefits of MSC transplantation may be associated with a paracrine modulatory effect and not only with a direct engraftment potential [43,47]. In particular, fetal MSCs have gained much attention as tools capable of activating the endogenous repair mechanisms of the host by furnishing a burst of paracrine factors [44,46]. Such an effect has been demonstrated despite their rapid clearance from the site of implantation and confirms that their physical existence at the site throughout the entire time required for repair to take place is not necessary to ensure complete healing. Furthermore, it has been shown that the secretome of these cells alone is capable of bringing about the same response [23,48]. The degree of stemness or level of lineage commitment of an MSC population appeared to directly influence this phenomenon. UC-MSCs, expressing low levels of typical embryonic stem cell (ESC) markers, such as POUF1, Nanog, Sox-2, and Lin28 [49], show a gene profile closer to ESCs [50], whereas BM-

MSCs express an osteogenic gene profile [24]. We observed that UC-MSC paracrine activity played a major role in the in vivo angiogenic effect elicited by implanted cells. The origin of the blood vessels was murine and no human cells differentiated into endothelial cells, indicating an indirect angiogenic effect rather than a direct differentiation of the cells. This was also confirmed by the fact that the UC-MSC secretome (CM) alone was capable of significantly inducing angiogenesis [49,51]. This effect was mediated only by UC-MSCs, excluding the possible role of endothelial progenitor contaminants as previously demonstrated [6].

Indeed, UC-MSCs have a secretome enriched with growth factors and cytokines related to angiogenesis, tissue repair, and wound healing processes when compared with BM-MSCs [52]. Many growth factors linked with angiogenesis were identified in the UC-MSC secretome, such as VEGF-D, PDGF-AA, TGF-β2, b-FGF, and HGF [53]. Interestingly, we also found that UC-MSCs secreted proinflammatory (CD40L, C5, and IL-6), proangiogenic (IL-6 and PAI-1), and chemotactic (CCL2, CCL5, IL-6, and IL-8) cytokines in high quantities [49,54]. IL-6 was recently associated with MSC pluripotency and immunoprivilege. The combination of BM-MSCs and IL-6 was shown to be much more effective in attenuating liver fibrosis than BM-MSCs alone [55]. These results suggest that UC-MSCs alone could be a more appropriate candidate for cell therapy since these cells secrete higher IL-6 levels [56].

Recent studies have highlighted the essential roles of proresolving M2 macrophages in tissue repair and regeneration [57]. We showed that UC-MSC secretome was enriched in M2 inducers, GM-CSF [58], CCL2, and IL-6 [59], thus suggesting a crucial role of the UC-MSC secretome in activating M2 proresolving macrophages, thereby modulating the wound healing process [26].

Despite their poor osteogenic capability when implanted ectopically, UC-MSCs were able to sustain the formation of new bone matrix in an orthotopic model in an amount comparable with that of implanted BM-MSCs [30,31]. It remains unclear if the in vivo paracrine effects of UC-MSCs are merely mediated by the UC-MSC secretome itself or also by an intercellular cross talk between the exogenous stem cells and the host endogenous progenitors; a new concept recently hypothesized in the literature [25].

In summary, the therapeutic potential of UC-MSCs appears to be vast and diverse and we are just beginning to discover their true potential. Although additional experiments are required to investigate further UC-MSC secretome-mediated angiogenesis in vivo, it can already be deduced from our study that UC-MSCs could have an effective potential use as an angiogenic tool. This is in addition to the immunomodulating role of the UC-MSC secretome making these cells, and/or their secretome, attractive therapeutic candidates for treatment of chronic wounds such as diabetic ulcers or nonhealing fractures.

Acknowledgments

The authors would like to thank Dr. Michele Cilli for the surgical assistance and Dr. Mauro Alini for providing the poly (ester urethane) scaffold. This work was partially supported by funds from Regione Liguria, Italy (POR-FESR 2007–2013).

Author Disclosure Statement

No competing financial interests exist.

References

1. Mauney JR, D Ph, V Volloch and DL Kaplan. (2005). Role of adult mesenchymal stem cells in bone tissue-engineering applications: current status and future prospects. Tissue Eng 11:787–802.
2. El Backly RM, SH Zaky, A Muraglia, L Tonachini, F Brun, B Canciani, D Chiapale, F Santolini, R Cancedda and M Mastrogiacomo. (2013). A platelet-rich plasma-based membrane as a periosteal substitute with enhanced osteogenic and angiogenic properties: a new concept for bone repair. Tissue Eng Part A 19:152–165.
3. Giannoni P, M Mastrogiacomo, M Alini, SG Pearce, A Corsi, F Santolini, A Muraglia, P Bianco and R Cancedda. (2008). Regeneration of large bone defects in sheep using bone marrow stromal cells. J Tissue Eng Regen Med 2:253–262.
4. Quarto R, M Mastrogiacomo, R Cancedda, SM Kutepov, V Mukhachev, A Lavroukov, E Kon and M Marcacci. (2001). Repair of large bone defects with the use of autologous bone marrow stromal cells. N Engl J Med 344:385–386.
5. Hass R, C Kasper, S Böhm and R Jacobs. (2011). Different populations and sources of human mesenchymal stem cells (MSC): a comparison of adult and neonatal tissue-derived MSC. Cell Commun Signal 9:12.
6. Capelli C, E Gotti, M Morigi, C Rota, L Weng, F Dazzi, O Spinelli, G Cazzaniga, R Trezzi, et al. (2011). Minimally manipulated whole human umbilical cord is a rich source of clinical-grade human mesenchymal stromal cells expanded in human platelet lysate. Cytotherapy 13:786–801.
7. Abu Kasim NH, V Govindasamy, N Gnanasegaran, S Musa, PJ Pradeep, TC Srijaya and ZA Aziz. (2012). Unique molecular signatures influencing the biological function and fate of post-natal stem cells isolated from different sources. J Tissue Eng Regen Med [Epub ahead of print]; DOI: 10.1002/term.1663.
8. El Omar R, J Beroud, J-F Stoltz, P Menu, E Velot and V Decot. (2014). Umbilical cord mesenchymal stem cells: the new gold standard for mesenchymal stem cell-based therapies? Tissue Eng Part B Rev 20:523–544.
9. Weiss ML, C Anderson, S Medicetty, KB Seshareddy, RJ Weiss, I VanderWerff, D Troyer and KR McIntosh. (2008). Immune properties of human umbilical cord Wharton's jelly-derived cells. Stem Cells 26:2865–2874.
10. Tipnis S, C Viswanathan and AS Majumdar. (2010). Immunosuppressive properties of human umbilical cord-derived mesenchymal stem cells: role of B7-H1 and IDO. Immunol Cell Biol 88:795–806.
11. Ribeiro A, P Laranjeira, S Mendes, I Velada, C Leite, P Andrade, F Santos, A Henriques, M Grãos, et al. (2013). Mesenchymal stem cells from umbilical cord matrix, adipose tissue and bone marrow exhibit different capability to suppress peripheral blood B, natural killer and T cells. Stem Cell Res Ther 4:125.
12. Che N, X Li, S Zhou, R Liu, D Shi, L Lu and L Sun. (2012). Umbilical cord mesenchymal stem cells suppress B-cell proliferation and differentiation. Cell Immunol 274:46–53.
13. Ji YR, ZX Yang, Z-B Han, L Meng, L Liang, XM Feng, SG Yang, Y Chi, DD Chen, YW Wang and ZC Han. (2012). Mesenchymal stem cells support proliferation and terminal

differentiation of B cells. Cell Physiol Biochem 30:1526–1537.
14. Wu Y, Y Cao, X Li, L Xu, Z Wang, P Liu, P Yan, Z Liu, J Wang, et al. (2014). Cotransplantation of haploidentical hematopoietic and umbilical cord mesenchymal stem cells for severe aplastic anemia: successful engraftment and mild GVHD. Stem Cell Res 12:132–138.
15. Deuse T, M Stubbendorff, K Tang-Quan, N Phillips, MA Kay, T Eiermann, TT Phan, H-D Volk, H Reichenspurner, RC Robbins and S Schrepfer. (2011). Immunogenicity and immunomodulatory properties of umbilical cord lining mesenchymal stem cells. Cell Transplant 20:655–667.
16. Introna M, G Lucchini, E Dander, S Galimberti, A Rovelli, A Balduzzi, D Longoni, F Pavan, F Masciocchi, et al. (2014). Treatment of graft versus host disease with mesenchymal stromal cells: a phase I study on 40 adult and pediatric patients. Biol Blood Marrow Transplant 20:375–381.
17. Dominici M, K Le Blanc, I Mueller, I Slaper-Cortenbach, F Marini, D Krause, R Deans, A Keating, D Prockop and E Horwitz. (2006). Minimal criteria for defining multipotent mesenchymal stromal cells. The International Society for Cellular Therapy position statement. Cytotherapy 8:315–317.
18. Majore I, P Moretti, F Stahl, R Hass and C Kasper. (2011). Growth and differentiation properties of mesenchymal stromal cell populations derived from whole human umbilical cord. Stem Cell Rev 7:17–31.
19. Girdlestone J, VA Limbani, AJ Cutler and C V Navarrete. (2009). Efficient expansion of mesenchymal stromal cells from umbilical cord under low serum conditions. Cytotherapy 11:738–748.
20. Suzdal'tseva YG, VV Burunova, IV Vakhrushev, VN Yarygin and KN Yarygin. (2007). Capability of human mesenchymal cells isolated from different sources to differentiation into tissues of mesodermal origin. Bull Exp Biol Med 143:114–121.
21. Bosch J, AP Houben, TF Radke, D Stapelkamp, E Bünemann, P Balan, A Buchheiser, S Liedtke and G Kögler. (2012). Distinct differentiation potential of ''MSC'' derived from cord blood and umbilical cord: are cord-derived cells true mesenchymal stromal cells? Stem Cells Dev 21:1977–1988.
22. Troyer DL and ML Weiss. (2008). Wharton's jelly-derived cells are a primitive stromal cell population. Stem Cells 26:591–599.
23. Schneider RK, A Puellen, R Kramann, K Raupach, J Bornemann, R Knuechel, A Pérez-Bouza and S Neuss. (2010). The osteogenic differentiation of adult bone marrow and perinatal umbilical mesenchymal stem cells and matrix remodelling in three-dimensional collagen scaffolds. Biomaterials 31:467–480.
24. Hsieh J and Y Fu. (2010). Functional module analysis reveals differential osteogenic and stemness potentials in human mesenchymal stem cells from bone marrow and Wharton's jelly of umbilical cord. Stem Cells Dev 19:1896–1910.
25. Bollini S, C Gentili, R Tasso and R Cancedda. (2013). The regenerative role of the fetal and adult stem cell secretome. J Clin Med 2:302–327.
26. Shohara R, A Yamamoto, S Takikawa, A Iwase, H Hibi, F Kikkawa and M Ueda. (2012). Mesenchymal stromal cells of human umbilical cord Wharton's jelly accelerate wound healing by paracrine mechanisms. Cytotherapy 14:1171–1181.
27. Muraglia A, I Martin, R Cancedda and R Quarto. (1998). A nude mouse model for human bone formation in unloaded conditions. Bone 22:131S–134S.
28. Ignowski JM and D V Schaffer. (2004). Kinetic analysis and modeling of firefly luciferase as a quantitative reporter gene in live mammalian cells. Biotechnol Bioeng 86:827–834.
29. Daga A, A Muraglia, R Quarto, R Cancedda and G Corte. (2002). Enhanced engraftment of EPO-transduced human bone marrow stromal cells transplanted in a 3D matrix in non-conditioned NOD/SCID mice. Gene Ther 9:915–921.
30. Kuiper EJ, P Roestenberg, C Ehlken, V Lambert, HB van Treslong-de Groot, KM Lyons, H-JT Agostini, J-M Rakic, I Klaassen, et al. (2007). Angiogenesis is not impaired in connective tissue growth factor (CTGF) knock-out mice. J Histochem Cytochem 55:1139–1147.
31. Spicer PP, JD Kretlow, S Young, JA Jansen, FK Kasper and AG Mikos. (2012). Evaluation of bone regeneration using the rat critical size calvarial defect. Nat Protoc 7:1918–1929.
32. Laschke MW, A Strohe, MD Menger, M Alini and D Eglin. (2010). In vitro and in vivo evaluation of a novel nanosize hydroxyapatite particles/poly(ester-urethane) composite scaffold for bone tissue engineering. Acta Biomater 6: 2020–2027.
33. (1997). Opinion of the EMEA on the potential risk associated with medicinal products in relation to bovine spongiform encephalopathy (BSE) (16 April 1996) and report from the Committee for Proprietary Medicinal Products (CPMP) on the'Note for Guidance on minimizing the risk of transmitting animal spongiform encephalopathies via medicinal products' (15 April 1997). Adverse Drug React Toxicol Rev 16:113–121.
34. Tuschong L, SL Soenen, RM Blaese, F Candotti and LM Muul. (2002). Immune response to fetal calf serum by two adenosine deaminase-deficient patients after T cell gene therapy. Hum Gene Ther 13:1605–1610.
35. Wang D, J Li, Y Zhang, M Zhang, J Chen, X Li, X Hu, S Jiang, S Shi and L Sun. (2014). Umbilical cord mesenchymal stem cell transplantation in active and refractory systemic lupus erythematosus: a multicenter clinical study. Arthritis Res Ther 16:R79.
36. Capelli C, M Domenghini, G Borleri, P Bellavita, R Poma, A Carobbio, C Micò, A Rambaldi, J Golay and M Introna. (2007). Human platelet lysate allows expansion and clinical grade production of mesenchymal stromal cells from small samples of bone marrow aspirates or marrow filter washouts. Bone Marrow Transplant 40:785–791.
37. Petsa A, S Gargani, A Felesakis, N Grigoriadis and I Grigoriadis. (2009). Effectiveness of protocol for the isolation of Wharton's Jelly stem cells in large-scale applications. In Vitro Cell Dev Biol Anim 45:573–576.
38. Majore I, P Moretti, R Hass and C Kasper. (2009). Identification of subpopulations in mesenchymal stem cell-like cultures from human umbilical cord. Cell Commun Signal 7:6.
39. Sotiropoulou PA, SA Perez, M Salagianni, CN Baxevanis and M Papamichail. (2006). Characterization of the optimal culture conditions for clinical scale production of human mesenchymal stem cells. Stem Cells 24:462–471.
40. Martin I, A Muraglia, G Campanile, R Cancedda and R Quarto. (1997). Fibroblast growth factor-2 supports ex vivo

expansion and maintenance of osteogenic precursors from human bone marrow. Endocrinology 138:4456–4462.
41. Chevallier N, F Anagnostou, S Zilber, G Bodivit, S Maurin, A Barrault, P Bierling, P Hernigou, P Layrolle and H Rouard. (2010). Osteoblastic differentiation of human mesenchymal stem cells with platelet lysate. Biomaterials 31:270–278.
42. Ohgushi H, J Miyake and T Tateishi. (2003). Mesenchymal stem cells and bioceramics: strategies to regenerate the skeleton. Novartis Found Symp 249: 118–127; discussion 127–132, 170–174, 239–241.
43. Mirabella T, A Poggi, M Scaranari, M Mogni, M Lituania, C Baldo, R Cancedda and C Gentili. (2011). Recruitment of host's progenitor cells to sites of human amniotic fluid stem cells implantation. Biomaterials 32:4218–4227.
44. Sabapathy V, B Sundaram, S Vm, P Mankuzhy and S Kumar. (2014). Human wharton's jelly mesenchymal stem cells plasticity augments scar-free skin wound healing with hair growth. PLoS One 9:e93726.
45. Mueller AA, N Forraz, S Gueven, G Atzeni, O Degoul, A Pagnon-Minot, D Hartmann, I Martin, A Scherberich and C McGuckin. (2014). Osteoblastic differentiation of Wharton jelly biopsy specimens and their mesenchymal stromal cells after serum-free culture. Plast Reconstr Surg 134:59e–69e.
46. Giannoni P, D Ph, S Scaglione, A Daga, C Ilengo, B Sci, M Cilli and R Quarto. (2010). Short-time survival and engraftment of bone marrow stromal cells in an ectopic model of bone regeneration. Tissue Eng Part A 16:489–499.
47. Prasanna SJ, D Gopalakrishnan, SR Shankar and AB Vasandan. (2010). Pro-inflammatory cytokines, IFNgamma and TNFalpha, influence immune properties of human bone marrow and Wharton jelly mesenchymal stem cells differentially. PLoS One 5:e9016.
48. Bianco P, X Cao, PS Frenette, JJ Mao, PG Robey, PJ Simmons and C-Y Wang. (2013). The meaning, the sense and the significance: translating the science of mesenchymal stem cells into medicine. Nat Med 19:35–42.
49. Fong C-Y, L-L Chak, A Biswas, J-H Tan, K Gauthaman, W-K Chan and A Bongso. (2011). Human Wharton's jelly stem cells have unique transcriptome profiles compared to human embryonic stem cells and other mesenchymal stem cells. Stem Cell Rev 7: 1–16.
50. Nagamura-Inoue T and H He. (2014). Umbilical cord-derived mesenchymal stem cells: their advantages and potential clinical utility. World J Stem Cells 6:195–202.
51. Tasso R, M Gaetani, E Molino, A Cattaneo, M Monticone, A Bachi and R Cancedda. (2012). The role of bFGF on the ability of MSC to activate endogenous regenerative mechanisms in an ectopic bone formation model. Biomaterials 33:2086–2096.
52. Hsieh J-Y, H-W Wang, S-J Chang, K-H Liao, I-H Lee, W-S Lin, C-H Wu, W-Y Lin and S-M Cheng. (2013). Mesenchymal stem cells from human umbilical cord express preferentially secreted factors related to neuroprotection, neurogenesis, and angiogenesis. PLoS One 8:e72604.
53. Balasubramanian S, P Venugopal, S Sundarraj, Z Zakaria, A Sen Majumdar and M Ta. (2012). Comparison of chemokine and receptor gene expression between Wharton's jelly and bone marrow-derived mesenchymal stromal cells. Cytotherapy 14:26–33.
54. Edwards SS, G Zavala, CP Prieto, M Elliott, S Martínez, JT Egaña, MR Bono and V Palma. (2014). Functional analysis reveals angiogenic potential of human mesenchymal stem cells from Wharton's jelly in dermal regeneration. Angiogenesis 17:851–866.
55. Nasir GA, S Mohsin, M Khan, S Shams, G Ali, SN Khan and S Riazuddin. (2013). Mesenchymal stem cells and Interleukin-6 attenuate liver fibrosis in mice. J Transl Med 11:78.
56. Amable PR, MVT Teixeira, RBV Carias, JM Granjeiro and R Borojevic. (2014). Protein synthesis and secretion in human mesenchymal cells derived from bone marrow, adipose tissue and Wharton's jelly. Stem Cell Res Ther 5:53.
57. Brancato SK and JE Albina. (2011). Wound macrophages as key regulators of repair: origin, phenotype, and function. Am J Pathol 178:19–25.
58. Grant V, AE King, E Faccenda and RW Kelly. (2005). PGE/cAMP and GM-CSF synergise to induce a pro-tolerance cytokine profile in monocytic cell lines. Biochem Biophys Res Commun 331:187–193.
59. Roca H, ZS Varsos, S Sud, MJ Craig, C Ying and KJ Pienta. (2009). CCL2 and interleukin-6 promote survival of human CD11b + peripheral blood mononuclear cells and induce M2-type macrophage polarization. J Biol Chem 284:34342–34354.

Address correspondence to:
Dr. Maddalena Mastrogiacomo
Department of Experimental Medicine (DIMES)
University of Genoa
IRCCS AOU San Martino-IST
National Cancer Research Institute
Largo Rosanna Benzi 10
Genova 16132
Italy

E-mail: maddalena.mastrogiacomo@unige.it

Received for publication October 15, 2014
Accepted after revision February 16, 2015
Prepublished on Liebert Instant Online February 16, 2015